Protein Science (1998), 7:2118–2126. Cambridge University Press. Printed in the USA.

Structural characterizations of nonpeptidic thiadiazole inhibitors of matrix metalloproteinases reveal the basis for stromelysin selectivity

B.C. FINZEL,[1] E.T. BALDWIN,[1] G.L. BRYANT, JR.,[1] G.F. HESS,[2] J.W. WILKS,[2] C.M. TREPOD,[3] J.E. MOTT,[3] V.P. MARSHALL,[4] G.L. PETZOLD,[4] R.A. POORMAN,[4] T.J. O'SULLIVAN,[5] H.J. SCHOSTAREZ,[5] AND M.A. MITCHELL[5]

[1]Structural, Analytical & Medicinal Chemistry, Pharmacia and Upjohn, Kalamazoo, Michigan 49007
[2]Cell & Molecular Biology, Pharmacia and Upjohn, Kalamazoo, Michigan 49007
[3]Bioprocess Research Preparations, Pharmacia and Upjohn, Kalamazoo, Michigan 49007
[4]Protein Science, Pharmacia and Upjohn, Kalamazoo, Michigan 49007
[5]Medicinal Chemistry, Pharmacia and Upjohn, Kalamazoo, Michigan 49007

(RECEIVED February 19, 1998; ACCEPTED June 24, 1998)

Abstract

The binding of two 5-substituted-1,3,4-thiadiazole-2-thione inhibitors to the matrix metalloproteinase stromelysin (MMP-3) have been characterized by protein crystallography. Both inhibitors coordinate to the catalytic zinc cation via an exocyclic sulfur and lay in an unusual position across the unprimed (P1–P3) side of the proteinase active site. Nitrogen atoms in the thiadiazole moiety make specific hydrogen bond interactions with enzyme structural elements that are conserved across all enzymes in the matrix metalloproteinase class. Strong hydrophobic interactions between the inhibitors and the side chain of tyrosine-155 appear to be responsible for the very high selectivity of these inhibitors for stromelysin. In these enzyme/inhibitor complexes, the S1′ enzyme subsite is unoccupied. A conformational rearrangement of the catalytic domain occurs that reveals an inherent flexibility of the substrate binding region leading to speculation about a possible mechanism for modulation of stromelysin activity and selectivity.

Keywords: collagenase; drug design; endopeptidase; gelatinase; matrix metalloproteinase; MMP

The matrix metalloproteinases (MMPs) are a family of zinc-dependent endopeptidases that degrade major components of extracellular connective tissue. While these enzymes are known to play important roles in tissue remodeling (Hulboy et al., 1997), wound healing (Fini et al., 1996), and development (Terada et al., 1997), the overexpression or faulty regulation of MMPs has been implicated in a number of degenerative diseases and inflammatory conditions including glaucoma (Snyder et al., 1993), periodontal disease (Ingman et al., 1993), arteriosclerosis (Newby et al., 1994), osteoarthritis (Serni et al., 1995), and emphysema (Finlay et al., 1997). Many tumors overexpress one or more MMPs (Matrisian, 1994). These enzymes are apparently involved in connective tissue degradation necessary for tumor metastasis and angiogenesis (Ray & Stetler-Stevenson, 1994; MacDougall & Matrisian, 1995), but they may also play a more complicated role in the regulation and growth of tumors and the development of metastatic disease (Chambers & Matrisian, 1997). It is hoped that broad spectrum inhibitors of the MMPs (MMPIs) will have therapeutic value in the treatment of cancer (Brown & Giavazzi, 1995).

Reprint requests to: Barry C. Finzel, Pharmacia and Upjohn, Kalamazoo, Michigan 49007; e-mail: Barry.C.Finzel@am.pnu.com.

The MMPs can be grouped into at least four subclasses by their sequence composition or substrate preferences and have been recently reviewed (Ray & Stetler-Stevenson, 1994; Chambers & Matrisian, 1997; Nagase, 1997). The collagenases (MMP-1, MMP-8, MMP-13) are most specific and preferentially degrade interstitial collagens (types I, II, and III). Gelatinases (MMP2, MMP9) and stromelysins (MMP-3, MMP-10, MMP-11) have broader specificity. Gelatinases degrade type IV collagen, fibronectin, and denatured collagen (gelatins). Stromelysins also degrade the protein core of proteoglycans. A subclass of "membrane-type" MMPs (MT-MMPs) possess an additional transmembrane domain. MT-MMPs play major roles in activating other MMPs. Generally, the MMPs are expressed as preproenzymes that include an N-terminal peptide segment signaling secretion, a pro segment that must be removed for enzyme activation, a catalytic domain, and a hemopexin-like domain (Nagase, 1997). The hemopexin domain is not necessary for proteolysis, but may be required for selection of native substrates. It has been suggested to be important for localization of MMP activity at the surface of invading cells.

The catalytic domain of the MMPs has been structurally characterized repeatedly. Crystal structures of collagenase (Bode et al., 1994; Borkakoti et al., 1994; Lovejoy et al., 1994a; Stams et al., 1994), matrilysin (Browner et al., 1995), and stromelysin (Becker

et al., 1995) catalytic domains have been reported. A structure of stromelysin including the inactivating pro-segment has been revealed (Becker et al., 1995), and there is one report of a full-length mature collagenase including a description of a propeller-like hemopexin domain (Li et al., 1995). All of these reports reveal a similar structure of the MMP catalytic domain recognizable as a five-stranded beta sheet with four parallel and one antiparallel beta strands, and three extended helices. All structures also include two tetrahedrally coordinated zinc ions. A "catalytic" zinc is coordinated by imidazole nitrogens of conserved histidines 201, 205, and 211 (stromelysin numbering), and to an inhibitor. This site is at the base of a substrate binding cleft where proteolysis occurs. A "structural" zinc, also coordinated by three histidines (151, 166, and 179) and the carboxyl oxygen of an aspartic acid residue (153), lies above the beta sheet 14 Å from the catalytic Zn^{+2}. As many as three calcium-binding sites have been characterized. Occupancy at these sites varies from MMP to MMP, and (in at least one case) with crystallization conditions (Lovejoy et al., 1994b).

Because of the obvious therapeutic potential for inhibitors of the MMPs, this class of enzymes has been the subject of a many independent efforts in inhibitor design. (See, for example, a recent review by Zask et al. (1996)). While some new nonpeptidic inhibitors are currently in the late stages of development, most of the structural literature reflects the earlier bias toward small peptide-mimetic inhibitors of the MMPs (Bode et al., 1994; Becker et al., 1995; Browner et al., 1995; Gowravaram et al., 1995; Grams et al., 1995; Dhanaraj et al., 1996; Esser et al., 1997). These inhibitors bind in a very well characterized manner, with either a hydroxamate or carboxylate zinc ligand at the N-terminal end of a short peptide-mimetic backbone that lies in the deep cleft across the S1′-S2′-(S3′) enzyme subsites. The structure-activity relationships among these inhibitors is now well established. Large hydrophobic substituents in the P1′ position can lead to increased potency for gelatinases and stromelysins, while selectively decreasing potency against collagenases. This selectivity is readily understood following inspection and comparison of enzyme catalytic domain structures. Longer peptidic moieties (spanning P1′–P3′) broadly inhibit MMPs, but physical characteristics of these compounds (solubility, serum half-life, oral absorption) are less than desirable as therapeutic agents. This understanding has more recently led to the discovery of a number of nonpeptidic inhibitors with better pharmacokinetic properties than can usually be achieved with peptidic templates (Zask et al., 1996). Still, the emphasis has generally been upon agents that bind in the S1′ subsite, an area of these enzymes that has proven a better site for development of selectivity than for broad-spectrum MMP inhibition.

We have been investigating a series of 5-substituted-1,3,4-thiadiazole-2-thiones as potentially novel, nonpeptidic alternatives to peptide-mimetic MMP inhibitors (Fig. 1). This series of compounds was identified by a screen of the Pharmacia and Upjohn compound collection for inhibitors of stromelysin (E.J. Jacobsen et al., in prep.). By systematically dissecting structure-activity relationships, medicinal chemists have identified several key structural requirements of these inhibitors: the unsubstituted exocyclic sulfur at the 2-position on the ring; the absence of any substituent on N^3H or N^4; an amino group attached to C^5. Further chemical SAR has demonstrated the advantages of either attached urea or amido groups as precursors to viable subclasses of compounds with improved affinity (Fig. 1). While significant progress has been made toward enhancing potency of this series against stromelysin (initial potency has been improved by 6,000-fold), such

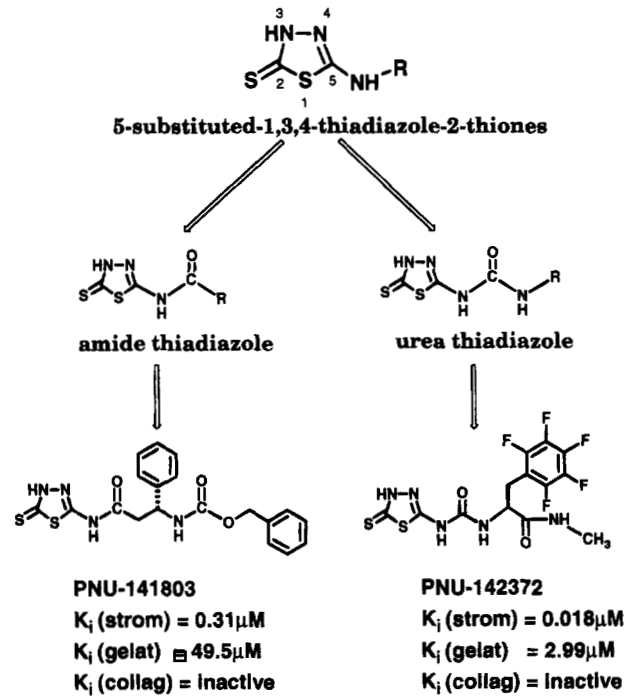

Fig. 1. Thiadiazole inhibitors of stromelysin and nomenclature to be used in this paper. Equilibrium binding constants (K_i) given for the two inhibitors quantitate affinities for stromelysin catalytic domain (strom), gelatinase A (gelat), and interstitial collagenase (collag) as described elsewhere (Jacobsen et al., 1998).

potency gains have not been achieved against other MMPs. Very few of the thiadiazoles have shown affinity for collagenase at detectable levels (~500 μM). Modeling studies have been frustrated by the fact that the thiadiazoles are so novel to this enzyme context, and the footprint of binding so unique. Available complexes with peptide mimetic inhibitors have little to offer to our understanding of the binding of the thiadiazoles.

Here we report the results of X-ray diffraction studies of two crystalline complexes of stromelysin catalytic domain and thiadiazole inhibitors (PNU-142372 and PNU-141803). The two inhibitors represent thiadiazoles of the urea and amide subclasses, respectively (Fig. 1). In addition to the urea attached directly to the thiadiazole, PNU-142372 incorporates a penta-fluorophenylalanine. This is one of the most potent analogs identified against stromelysin (K_i = 0.018 μM). PNU-141803 (K_i = 0.27 μM) is a member of the amide-thiadiazole series (H.J. Schostarez et al., in prep.). It includes a β-phenylalanine and an attached O-benzylcarbamate. Both compounds show limited activity against gelatinase-A and none at all against collagenase (Fig. 1). With this work we hope to establish a structural basis for understanding this selectivity.

Results and discussion

We have determined the structures of two stromelysin/thiadiazole inhibitor complexes at high (1.6 Å) to moderate (2.2 Å) resolution (see Table 1). Both complexes exist in the same heretofore undescribed rhombohedral crystal form. The stromelysin catalytic domain structures resulting from this work are similar to those reported elsewhere with different inhibitors (Becker et al., 1995;

Table 1. *Crystallographic data and refinement statistics*

	PNU-142372 complex	PNU-141803 complex
Maximum resolution	1.6 Å	2.2 Å
No. of observations collected	96250	38781
No. of unique reflections	20522	8566
Percentage of total reflections	95%	88%
R_{sym}	7.5%	8.6%
Cell constants (Å)		
a,b,c (rhombohedral cell)	75.16 Å	75.06 Å
α,β,γ (rhombohedral cell)	56.28°	56.16°
a,b (hexagonal cell)	72.12 Å	70.89 Å
c (hexagonal cell)	192.06 Å	189.11 Å
Intermediate refinement results	R-value	R-value
Replacement solution (6.0–3.5 Å)	0.417	0.305
Rigid body refinement (5.0–2.5 Å)	0.379	0.256
SA refinement (8.0–2.0 Å)	0.295	Not needed
XPLOR positional refinement	0.246 (8–2.0 Å)	0.207 (8–2.5 Å)
Final model refinement statistics		
Reflection subset used in refinement ($F_{obs} \geq 2\sigma_F$)	10–1.8 Å	10.0–2.2 Å
Final R-value	0.189	0.172
No. of reflections used	17,046	8,429
% of possible reflections used	94% (10–1.8 Å) 85% (1.8–1.9 Å)	88% (10–2.2 Å) 82% (2.2–2.3 Å)

Dhanaraj et al., 1996) or in solution (Gooley et al., 1994). Two Zn^{+2}-binding sites and three Ca^{+2}-binding sites are occupied as reported elsewhere (Becker et al., 1995). A third Zn^{+2}-binding site, apparently unique to this rhombohedral crystal form, is also observed. It lies on the crystallographic threefold axis where it is coordinated by three symmetry-related instances of His96, a side chain normally found exposed at the molecular surface. A fourth ligand for this ion, completing the tetrahedral coordination sphere, also lies exactly on the threefold axis. The electron density is consistent with speculation that this fourth ligand is a carbonate ion, but no firm evidence supports this assignment.

The two stromelysin-thiadiazole inhibitors characterized here bind on the more open "unprimed" side of the enzyme catalytic site, across a region occupied by the backbone of a substrate lying in the S1–S3 enzyme subsites. This region of the substrate binding cleft of stromelysin has not been exhaustively described. Only one P1–P3 inhibitor of collagenase, a Pro-Leu-Gly-hydroxamate, has been structurally characterized by others (Bode et al., 1994). In contrast to the primed side (S1′–S3′), which has a well-defined S1′ pocket, the unprimed side consists of larger open spaces and shallow hydrophobic potholes (Fig. 2). The S1 and S3 subsites are actually combined into one large open space (S1/S3) bounded by backbone and side-chain atoms of His166, Ala167, and Tyr168 at the back, and the side chain of Tyr155 at the top (see Fig. 2 for orientational reference). Side chains of His205, Phe210, and Phe86 assemble to form a shallow depression that is the S2 "pocket." A similar depression at the intersection of Phe86, Pro87, Pro90, and Ala169 side chains is S4.

Thiadiazole binding

The inhibitors are coordinated to the catalytic zinc cation via the exocyclic sulfur of the thiadiazole. The Zn^{+2}-S-C bond angle is approximately 90°. The planar thiadiazole and attached coplanar amide (or urea) common to both inhibitors lie flat along the floor of the broad trough of S1-S3. Heteroatoms along the perimeter of the conjugated ring system complement and interact with the extended backbone of β4 that lines the inside edge of the trough, while the hydrophobic underside of the thiadiazole covers the shallow S2 subsite supported by side chains of Phe86 and Phe210. Specific heteroatom interactions between stromelysin and each inhibitor are summarized in the schematic diagrams of Figure 3. The two molecules share many common interactions. The hydrogen on N^3 (the thiadiazole ring nitrogen closest to the exocyclic sulfur) makes a bifurcated hydrogen bond to the carboxylate oxygens of Glu202. This glutamate is conserved in all the zinc-peptidases (Stöcker et al., 1995), and likely plays a crucial role in catalysis (Matthews, 1988; Becker et al., 1995). The other ring nitrogen accepts a hydrogen bond from the backbone amide of Ala167. The five-amide substituent of the ring is positioned ideally to donate a hydrogen bond to the Ala167 backbone carbonyl. All of these thiadiazole heteroatoms were thought to play a significant role in binding because of chemical SAR. Analogs with any substitution at N^3 are inactive, as are any thiadiazoles that lack the exocyclic sulfur (E.J. Jacobsen et al., in prep.). The amide carbonyl is also required for potency in this class (E.J. Jacobsen et al., in prep.). These dependencies are explained easily in light of the crystal structure. Substitution of any one of these nitrogens with carbon not only eliminates a key hydrogen bond, but also presents a steric hindrance to the optimization of all the other hydrogen bonds.

The endocyclic sulfur does not appear to interact with any protein group, but is also necessary for activity (E.J. Jacobsen et al., in prep.). It is likely required for electronic delocalization of charge in the thiadiazole ring, which is necessary for Zn^{+2} coordination. The carbonyl of the amide substituent in both complexes points away from the enzyme and interacts only with water. The coplanarity of the entire fused thiadiazole-amide substructure may help enhance binding to the beta strand.

Beyond the amide, however, the inhibitor structures begin to differ, and the differences are reflected in the bound geometry. The urea of PNU-142372 makes a second interaction with the carbonyl of Ala167 (Fig. 4). This carbonyl is positioned perfectly to hydrogen bond to the diamide of the urea, optimizing both electrostatic interactions and surface complimentarity. Since the amide of PNU-141803 lacks the second heteroatom of the urea, the molecule twists above the plane of the beta-strand to avoid a close carbon-oxygen nonbonded contact (Fig. 4). Both molecules eventually reconverge onto a common position to present a carbonyl for interaction with the beta strand amide at Ala169; the methyl amide carbonyl of PNU-142372 and the carbamate carbonyl of PNU-141803 lie in the same position in superimposed complexes (Fig. 2). Because the urea of PNU-142372 maintains coplanarity with the beta strand, the carbonyl position can be reached with an inhibitor that is one carbon shorter.

The hydrogen bond interactions described above are common to both inhibitors, and while these are necessary to the design of thiadiazole-based inhibitors, they are apparently not sufficient. Many analogs have been synthesized that include all of the above functional groups but retain only limited affinity for MMPs (E.J. Jacobsen et al., in prep.; H.J. Schostarez et al., in prep.). Moreover,

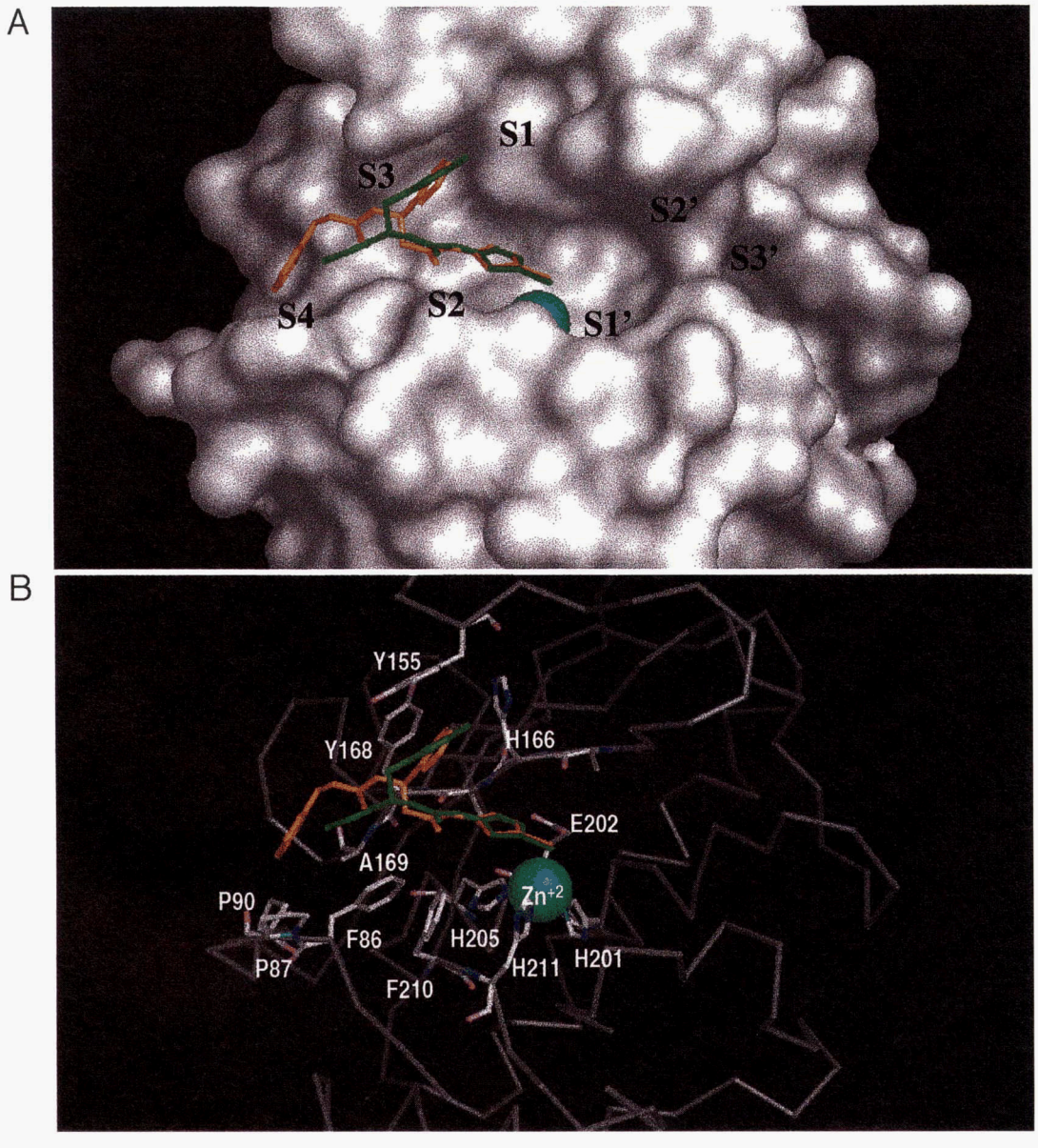

Fig. 2. The stromelysin inhibitor-binding cleft and underlying molecular structure. Above, an accessible surface of the stromelysin active site with bound thiadiazole inhibitors PNU-142372 (green) and PNU-141803 (orange). Enzyme subsites (S4–S1, S1′–S3′) are identified for convenience of discussion. The underlying atomic structure of the S4–S1 subsites are illustrated in the view below. The enzyme structure from the PNU-142372 complex is illustrated.

all of these interactions involve enzyme structural features that are common to entire families of MMPs. Structural homologues of backbone atoms of β4 (stromelysin residues 166–169) exist in nearly identical positions in collagenase, for example, as does the conserved side chain of Glu202. Models of collagenase/thiadiazole complexes can be easily contrived that include all of the same hydrogen bonds discussed above. Nevertheless, these stromelysin inhibitors show no measurable affinity for collagenase. Other hydrophobic interactions must be responsible for this selectivity.

PNU-142372 exhibits very highly optimized hydrophobic interactions. The pentafluorophenyl substituent forks from the thiadiazole-urea template at a position analogous to a side chain of the P3 position of a hypothetical peptidic inhibitor. From this position, it adopts an orientation that allows it to lie flat alongside the side chain of Tyr155, thereby optimizing a π-π stacking interaction (Fig. 4). A similar orientation can be envisioned for nonfluorinated analogs of this compound, but synthesis of a simple phenyl analog of PNU-142372 has led to a compound with 40-fold lower potency for stromelysin ($K_i = 0.71\ \mu$M) (E.J. Jacobsen et al., in prep.). The pentafluoro group is necessary for high affinity of this inhibitor. The meta and para fluorines of the pentafluoro-phenyl substituent interact with a protein-bound water molecule that is itself bound to conserved His166 Nδ_1. Like the interaction of the urea and Ala167 carbonyl, this interaction represents an optimization of both electrostatic interactions and surface complimentarity. This water molecule binding site is conserved in all MMPs, and has been occupied

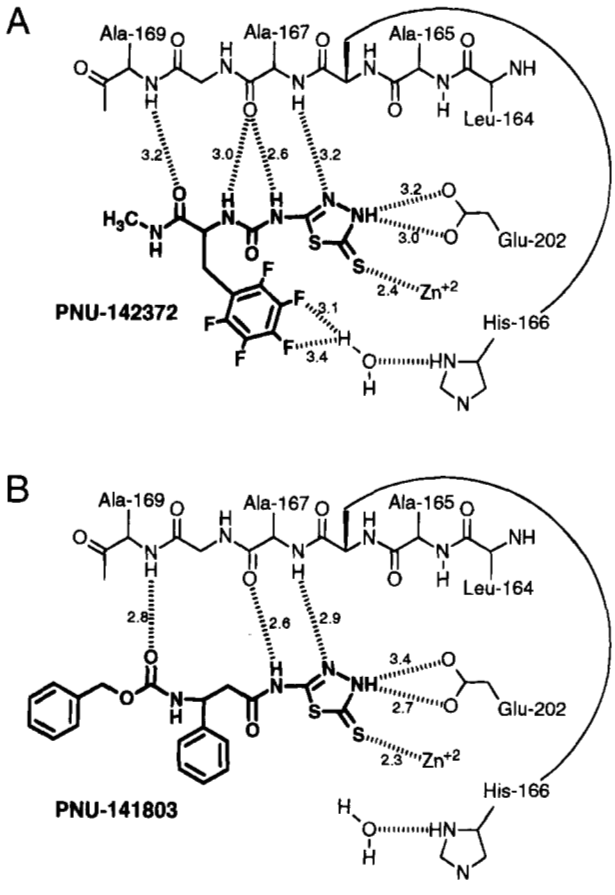

Fig. 3. Hydrogen bonding between thiadiazole inhibitors and the stromelysin active site. **A:** PNU-141372 complex. **B:** PNU-141803 complex. Interatomic distances given (in Ångstroms) are those observed between protein and inhibitor heteroatoms. Hydrogen positions must be inferred from heavier atom positions.

in every MMP structure reported to date. The presence of other fluorines on the ring may electronically enhance the π-π stacking interaction with Tyr155, perhaps accounting for slower ring flip rates observed spectroscopically for PNU-142372 (Stockman et al., 1998), and also contributing to enhanced binding affinity.

The hydrophobic interactions with PNU-141803 are not so highly idealized. The β-phenylalanine side chain branches from a slightly different position and with different geometry, so that the phenyl group points at Tyr155, but does not stack alongside it (Fig. 4). As a result, there are fewer hydrophobic interactions between this tyrosine and the inhibitor. The absence of π-π stacking is the simplest explanation for the much lower affinity of PNU-141803 for the enzyme. Still, it is likely that hydrophobic condensation against the Tyr155 side chain plays a big part in stabilizing the binding of both inhibitors. The O-benzylcarbamate at the far end of PNU-141803 reaches all the way to the S4 subsite of the enzyme, but this pocket is very shallow. One meta-carbon of the benzyl group makes a single hydrophobic contact with Cγ of Pro90, but this substituent does not appear well optimized.

Several differences exist between MMP structures that help to explain the poor affinity of these inhibitors for collagenase. Neither Phe86 (S2, S4) or Pro87 (S4) have homologues in collagenase, because these residues are part of an N-terminal extension of the mature catalytic domain that is unique to stromelysin. Phe210 is replaced with a serine or alanine in collagenase (Stöcker et al., 1995). The side chains of Phe86 and Phe210 are juxtaposed in stromelysin to form the shallow P2 subsite that supports the bound thiadiazole ring (Fig. 5). In collagenase, this hydrophobic S2 platform is absent, creating a much larger substrate binding cleft. Without Tyr155 (a serine in all collagenases), no π-π interactions with an inhibitor are possible. These structural differences cooperate to make the entire P1–P3 enzyme binding site much wider and more hydrophilic (Fig. 5). The Ala169-Gln change likewise works against thiadiazole binding, because the larger glutamine side chain in this position denies access to the backbone amide of Ala169 (Fig. 5). All of the thiadiazole inhibitors with submicromolar stromelysin affinity have a functional group that can hydrogen bond to Ala169 (Jacobsen et al., 1998). We conclude that S1–S3 is not a good target for mutual inhibition of stromelysin and collagenase, and it is probably not a good target for inhibition of collagenase by any inhibitor template.

No structure of gelatinase, the third and perhaps most important MMP therapeutic target in oncology, has been reported. It has been possible to develop potent inhibitors of gelatinase however, in part because of close parallels with the SAR of stromelysin. (For examples, see Zask et al., 1996). These are primarily P1′–P3′ inhibitors, and from this it is reasonable to conclude that there are strong similarities between S1′–S3′ enzyme subsites in gelatinase and stromelysin. Thiadiazole affinities for stromelysin are not paralleled in gelatinase, suggesting that stromelysin does not provide an effective model of the gelatinase S1–S3 subsites.

Comparison to other stromelysin/inhibitor complexes

The enzyme structures reported here are very similar to those reported elsewhere (Becker et al., 1995); the root-mean-square (RMS) difference in all alpha carbon positions following superposition is 1.06 Å. Nevertheless, there are some significant differences. The rhombohedral crystal form obtained from thiadiazole inhibited enzyme is unique. The C-terminally truncated catalytic domain (83–247) can be accommodated within this symmetry, while constructs with longer C-terminal extensions cannot because of packing constraints. We have not been successful in attempts to reproduce this crystal form, even with this same construct, with inhibitors belonging to other structural classes. The turn connecting β5 and α2 (residues 188–192) adjusts to a different conformation in the rhombohedral crystals to optimize nonspecific contacts with a thiadiazole inhibitor bound to another enzyme molecule related by crystallographic symmetry. These interactions may be necessary to the formation of this crystal form.

The largest differences in conformation of the stromelysin catalytic domain, between earlier reports and the complexes described, here are found in the residues that form the floor of the right side of the substrate binding cleft—away from the thiadiazole inhibitor binding site. In the absence of an inhibitor with a P1′ substituent, Tyr223 shifts more than 7 Å from a position on the right wall of the S1′ pocket, to a new position buried squarely within S1′, actually adopting the position shared by many large aromatic P1′ substituents seen in enzyme/inhibitor complexes. This is not accomplished by simple reorientation of the side chain, but requires an accompanying 3–4 Å shift of the backbone (Fig. 6). To affect this change, the subsequent residues must also shift to the left, giving rise to an entirely different conformation. This "S1′-closed" conformation also has been observed in an un-

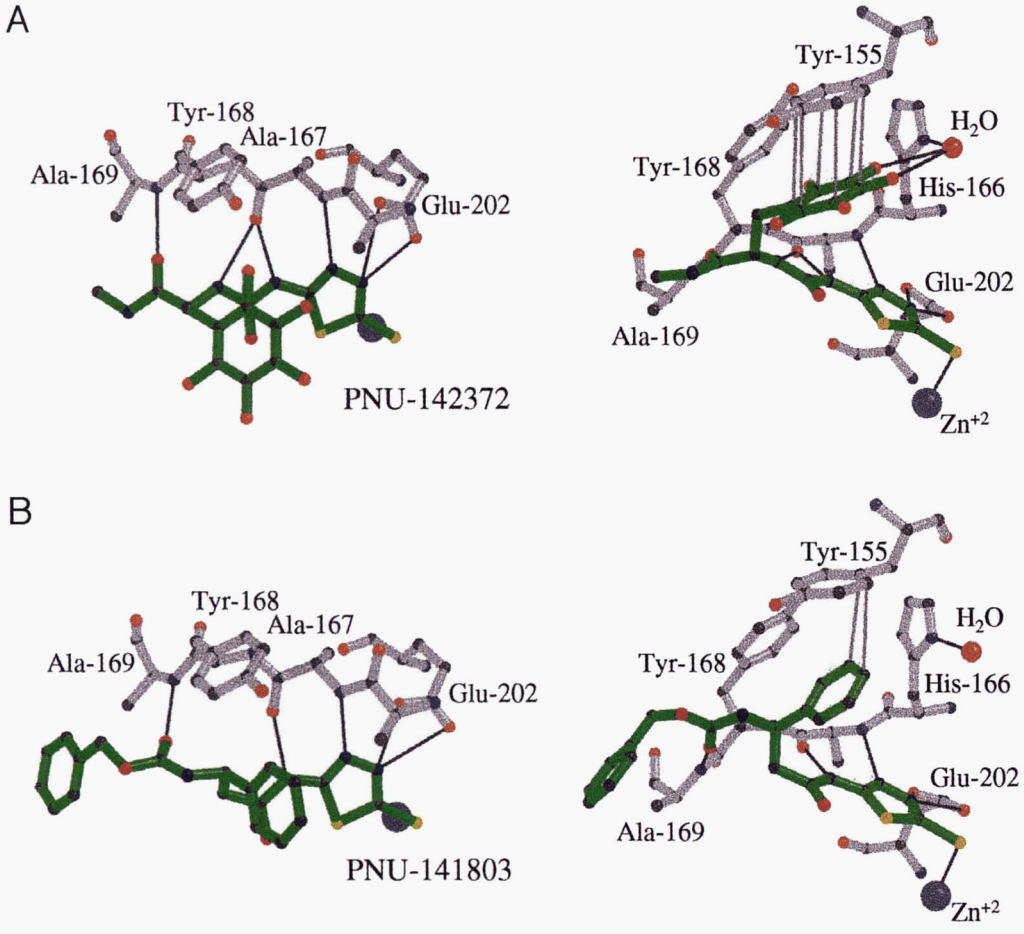

Fig. 4. Details on inhibitor binding geometry and interactions between the enzyme (white) and inhibitors (green) (**A**) PNU-142372 and (**B**) PNU-141803 (below). Two roughly orthogonal views of each complex are shown: at left, highlighting interactions between the thiadiazole inhibitors and the outside exposed edge of β4; at right, viewed along the edge of the inhibitors and the β-strand. Hydrogen bonds are illustrated with thin solid lines. Additional hydrophobic contacts (3.8–4.0 Å) between the P3 aromatic group of the inhibitor and Tyr155 are shown in the left view (lighter thin lines). These figures were prepared with Molscript (v 1.4) (Kraulis, 1991) and raster3d (v 2.1) (Merritt & Murphy, 1994).

inhibited stromelysin catalytic domain structure determined in our laboratory (B.C. Finzel, unpubl. data), but in that case residues 224–229 are mostly disordered. Here, the unusual conformation may be immobilized beneath intimate crystal contacts that stabilize this unique conformation. The existence of a large, hydrophobic S1′ pocket is certainly supported by extensive SAR, including many enzyme/inhibitor complex crystal structures, that have confirmed S1′ occupation by moieties ranging in size from an isobutyl hydrocarbon to large substituted biphenyls (Zask et al., 1996). The "S1′-open" conformation still appears to be the most realistic active site configuration for structure-based drug design.

The difference between S1′-closed and S1′-open conformations represents extremes that illustrate an inherent flexibility with potential importance to substrate specificity and drug design. Besides rearranging in response to inhibitor binding, this region is susceptible to changes to accommodate alternate crystal packing geometry, and has been described as flexible in solution (P. Yuan & B.J. Stockman, in prep.). This flexibility may be an artifact of the isolated stromelysin catalytic domain. In a report of the structure of full-length porcine collagenase, Li et al. (1995) have shown that the hemopexin domain of collagenase associates with the catalytic domain at an interface that includes residues homologous to 223–227 in stromelysin. The position of the hemopexin domain in full-length stromelysin has not been experimentally determined, but some homology to collagenase can be expected and a common hemopexin domain interface might exist. There is an unusual clustering of exposed hydrophobic amino acid residues on the stromelysin molecular surface, including Tyr220, His224, Leu226, and Phe232, that might define the perimeter of this hemopexin binding site (Fig. 6). These residues could identify a hydrophobic resting place for the stromelysin hemopexin domain that, if present, would constrain the conformation of the underlying polypeptide chain of residues 223–229, potentially modulating the conformational state of the P1′ pocket and thereby the affinity of the enzyme for certain substrates. It is interesting to speculate if this might be a part of the mechanism by which the hemopexin domain confers specificity for matrix substrates.

Materials and methods

The detailed synthesis of inhibitors PNU-142372 and PNU-141803 will be described elsewhere (E.J. Jacobsen et al., in prep.; H.J. Schostarez et al., in prep.).

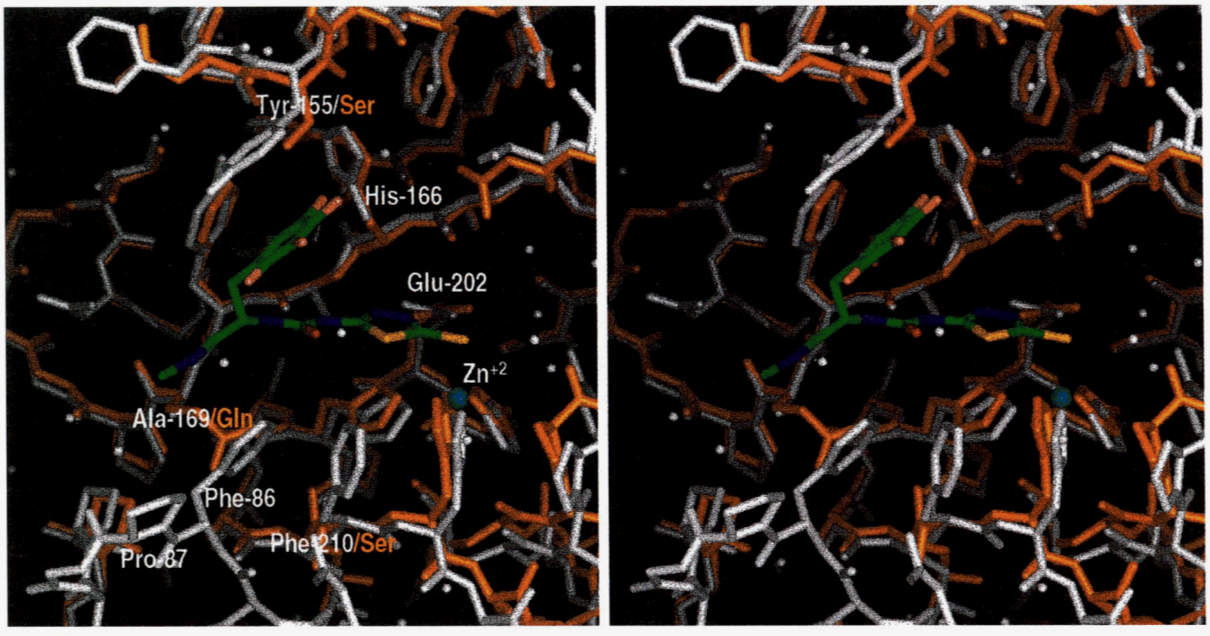

Fig. 5. Comparison of collagenase and stromelysin structures in the vicinity of the thiadiazole inhibitor binding site. The stromelysin structure from the PNU-142372 complex is shown (white) overlayed on human fibroblast collagenase (orange) (Spurlino et al., 1994). Sequence substitutions important to the stromelysin selectivity of the thiadiazoles include Ala169/Gln, Tyr155/Ser, and Phe210/Ser.

Full length stromelysin cDNA was obtained from M. Kurkinen (University of Medicine and Dentistry of New Jersey) (Saus et al., 1988). The gene encoding the pro segment and catalytic domain (residues 1–247) was cloned into a pET-11 plasmid (Novagen) and transformed into *Escherichia coli* expression strain BL21(DE3) (Novagen) following the strategy of Marcy et al. (1991). Insoluble proenzyme was extracted from lysed cell paste into 6 M urea, renatured by dialysis against 10 mM Bicine, 5 mM $CaCl_2$, 5 mM $ZnCl_2$, 0.02% NaN_3, pH 8.0, and purified by Q-Sepharose anion exchange chromatography (Marcy et al., 1991). Inactive proenzyme was activated by heating at 55 °C for 2.5 h, which catalyzes autodegradation of the pro segment (residues 1–82) leaving intact, active stromelysin catalytic domain (83–247) (Wetmore & Hardman, 1996). Digested pro segment fragments were removed by ultrafiltration. The yield was typically 3–4 mg of purified activated enzyme per liter of induced cells.

Activated enzyme was dialyzed into 10 mM HEPES; pH 7.5; 5 mM $CaCl_2$; 2 mM $ZnCl_2$; 0.02% NaN3; and concentrated by ultracentrifugation to 14.8 mg/mL in preparation for crystallization. Small aliquots (0.30 mL) of protein solution were inhibited

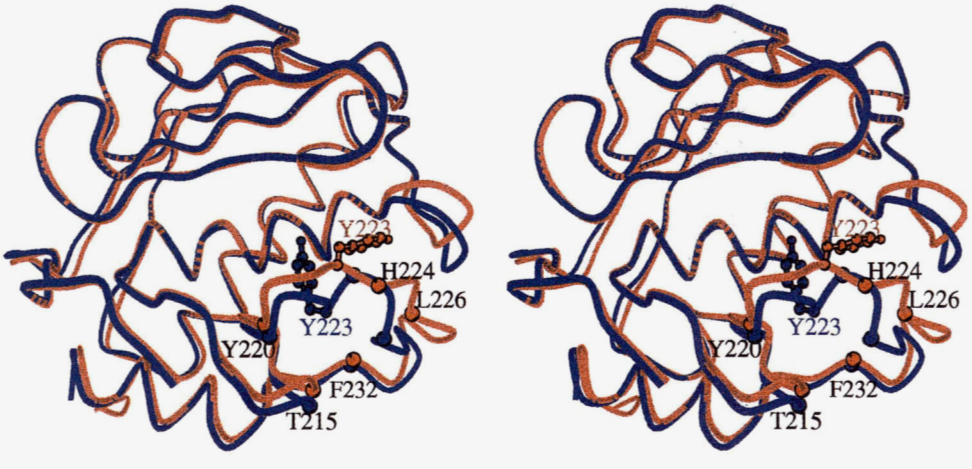

Fig. 6. A stereoscopic comparison of the structures of stromelysin in complex with the thiadiazoles (blue; this work), and a previous P1′-P2′-binding peptide-mimetic inhibitor (orange) (Becker et al., 1995). The change in the position of Tyr223 is illustrated. To effect this change, much of the adjoining loop segment (residues 224–231) must adjust conformation also. The α-carbon positions of several exposed hydrophobic residues (Thr215, Tyr220, His224, Leu226, Phe232) are shown to identify a region of stromelysin postulated to bind to the hemopexin domain.

by slow addition of 4 μL of PNU-142372 in 100% PEG400 (25 mg/mL) with mixing. The complex was spun down without any noticeable production of precipitate. Crystallization conditions were screened using an incomplete factorial design with PEG 6000 as the precipitant. Two microliters of inhibited protein were mixed with two microliters of buffered PEG/salt solution and placed on a micro-bridge in a 24 well Linbro plate and sealed for vapor equilibration. Large, single hexagonal bi-pyramid crystals grew from 0.1 M $LiSO_4$; 0.1 M Li Hepes pH 7.0; 20–25% PEG 6000; in one week.

Other small lots of stromelysin inhibited with PNU-141803 were prepared as needed for crystallization trials. An inhibitor solution (10 mM PNU-141803 in 100% DMSO) was added to protein (13 mg/mL) in a ratio of 1:10 (1 μL inhibitor to 10 μL protein, etc.) as above. The very successful PNU-142372/stromelysin complex conditions were tried first. After about 2 weeks, a few very small micro-crystals were observed in 22.5% PEG 6000. Microcrystals were diluted and serially passed through fresh drops. Small crystals appeared after about 1 month. These crystals tend to favor a hexagonal plate-like morphology but are isomorphous with the PNU-142372 crystals. Crystals exceeding 0.2 mm in the largest dimension were obtained by a third cycle of seeding.

Diffraction data for each complex were collected at room temperature using a Siemens Dual HiStar area detector system, and processed with XENGEN software (Howard et al., 1987). Observed unit cell parameters for the two complexes described herein are shown in Table 1. Crystals reflect the symmetry of space group R32. Rhombohedral cell edges were transformed by [−1 0 1; 1 −1 0; 1 1 1] to yield a corresponding hexagonal cell choice. Except for data processing, all subsequent calculations were performed upon the hexagonal unit cell. The approximate unit cell dimensions, $a = b = c = 72$ Å, $\alpha = \beta = \gamma = 56°$, allow for just one catalytic domain per asymmetric unit.

The structure of the PNU-142372 complex was determined first. Initial phases were obtained by application of molecular replacement techniques in the XPLOR program package (Brünger, 1992). A search model, consisting of all protein and bound cations from a stromelysin model available in an electronic appendix of Becker et al. (1995), was used to compute a cross rotation function from 4.0–8.0 Å. The top 125 peaks from this function were filtered with PC-refinement (Brünger, 1990). The highest rotation function peak also resulted in the highest PC-filtered peak at PC = 0.0864. The position of the rotated molecular model was then obtained by translational search. The highest peak in the translation function (14.3σ) reflected an excellent solution with good packing and an R-value for all data in the range 6.0–3.5 Å of 0.42.

The model was first refined as a single rigid body with XPLOR. Adjustments were then made to the model as required to fit initial electron density, with emphasis on conformational changes necessary to accommodate the rhombohedral symmetry. A single round of simulated-annealing (SA) refinement (XPLOR) was then applied to sharply reduce the R-factor, and the model regularized with positional and temperature factor refinement. Difference maps were then examined for evidence of inhibitor binding and an idealized model for the inhibitor was fit to this density. Positional and isotropic temperature factor refinement was completed with the restrained least squares of PROLSQ (Hendrickson & Konnert, 1980). Further adjustments to the model were made as suggested upon examination of $2F_o - F_c$ and $F_o - F_c$ difference maps. Bound water molecules were added to the model only if positive $F_o - F_c$ density (3σ level) and H-bonding allowed unambiguous identification. The refinement progress and final model agreement statistics are summarized in Table 1.

The structure of the PNU-141803/stromelysin complex was solved similarly, using the final coordinates from the PNU-142372/SLN structure solution (without inhibitor or solvent) as the search probe. No XPLOR SA refinement was performed upon this model.

Atomic coordinates for both PNU-142372 and PNU-141803 complexes have been deposited with the Protein Data Bank (Bernstein et al., 1977) along with supplementary data that may aid in the evaluation of the quality of the molecular model (PDB-ID 1usn and 2usn).

References

Becker JW, Marcy AI, Rokosz LL, Axel MG, Burbaum JJ, Fitzgerald PM, Cameron PM, Esser CK, Hagmann WK, Hermes JD, Springer JP. 1995. Stromelysin-1: Three-dimensional structure of the inhibited catalytic domain and of the C-truncated proenzyme. *Protein Sci 4*:1966–1976.

Bernstein FC, Koetzle TF, Williams GJB, Meyer EF Jr, Brice MD, Rodgers JR, Kennard O, Shimanouchi T, Tasumi M. 1977. The Protein Data Bank: A computer-based archival file for macromolecular structures. *J Mol Biol 112*:535–542.

Bode W, Reinemer P, Huber R, Kleine T, Schnierer S, Tschesche H. 1994. The X-ray crystal structure of the catalytic domain of human neutrophil collagenase inhibited by a substrate analogue reveals the essentials for catalysis and specificity. *EMBO J 13*:1263–1269.

Borkakoti N, Winkler FK, Williams DH, D'Arcy A, Broadhurst MJ, Brown PA, Johnson WH, Murray EJ. 1994. Structure of the catalytic domain of human fibroblast collagenase complexed with an inhibitor. *Nat Struct Biol 1*:106–110.

Brown PD, Giavazzi R. 1995. Matrix metalloproteinase inhibition: A review of anti-tumor activity. *Ann Oncol 6*:967–974.

Browner MF, Smith WW, Castelhano AL. 1995. Matrilysin-inhibitor complexes: Common themes among metalloproteases. *Biochemistry 34*:6602–6610.

Brünger AT. 1990. Extension of molecular replacement: A new search strategy based on Patterson correlation refinement. *Acta Crystallogr A 46*:46–57.

Brünger AT. 1992. *X-PLOR Version 3.1, A system for X-ray crystallography and NMR*. New Haven, CT: Yale University Press.

Chambers AF, Matrisian LM. 1997. Changing views of the role of matrix metalloproteinases in metastasis. *J Natl Cancer Inst 89*:1260–1270.

Dhanaraj V, Ye QZ, Johnson LL, Hupe DJ, Ortwine DF, Dunbar JB Jr, Rubin JR, Pavlovsky A, Humblet C, Blundell TL. 1996. X-ray structure of a hydroxamate inhibitor complex of stromelysin catalytic domain and its comparison with members of the zinc metalloproteinase superfamily. *Structure 4*:375–386.

Esser CK, Bugianesi RL, Caldwell CG, Chapman KT, Durette PL, Girotra NN, Kopka IE, Lanza TJ, Levorse DA, MacCoss M, Owens KA, Ponpipom MM, Simeone JP, Harrison RK, Niedzwiecki L, Becker JW, Marcy AI, Axel MG, Christen AJ, McDonnell J, Moore VL, Olszewski JM, Saphos C, Visco DMSF, Colletti A, Krieter PA, Hagmann WK. 1997. Inhibition of stromelysin-1 (MMP-3) by P1′-biphenylylethyl carboxyalkyl dipeptides. *J Med Chem 40*:1026–1040.

Fini ME, Parks WC, Rinehart WB, Girard MT, Matsubara M, Cook JR, West Mays JA, Sadow PM, Burgeson RE, Jeffrey JJ, Raizman MB, Krueger RR, Zieske JD. 1996. Role of matrix metalloproteinases in failure to re-epithelialize after corneal injury. *Am J Pathol 149*:1287–1302.

Finlay GA, Russell KJ, McMahon KJ, D'arcy EM, Masterson JB, FitzGerald MX, O'Connor CM. 1997. Elevated levels of matrix metalloproteinases in bronchoalveolar lavage fluid of emphysematous patients. *Thorax 52*:502–506.

Gooley PR, O'Connell JF, Marcy AI, Cuca GC, Salowe SP, Bush BL, Hermes JD, Esser CK, Hagmann WK, Springer JP, Johnson BA. 1994. The NMR structure of the inhibited catalytic domain of human stromelysin-1. *Nat Struct Biol 1*:111–118.

Gowravaram MR, Tomczuk BE, Johnson JS, Delecki D, Cook ER, Ghose AK, Mathiowetz AM, Spurlino JC, Rubin B, Smith DL, Pulvino T, Wahl RC. 1995. Inhibition of matrix metalloproteinases by hydroxamates containing heteroatom-based modifications of the P1′ group. *J Med Chem 38*:2570–2581.

Grams F, Crimmin M, Hinnes L, Huxley P, Pieper M, Tschesche H, Bode W. 1995. Structure determination and analysis of human neutrophil collagenase complexed with a hydroxamate inhibitor. *Biochemistry 34*:14012–14020.

Hendrickson WA, Konnert JH. 1980. Incorporation of stereochemical information into crystallographic refinement. In: Diamond R, Ramaseshan S, Vent-

katesan K, eds. *Computing in crystallography*. Bangalore, India: Indian Academy of Science. pp 13.01–13.25.

Howard AJ, Gilliand GL, Finzel BC, Poulos TL, Ohlendorf DH, Salemme FR. 1987. The use of an imaging proportional counter in macromolecular crystallography. *J Appl Crystallogr 20*:383–387.

Hulboy DL, Rudolph LA, Matrisian LM. 1997. Matrix metalloproteinases as mediators of reproductive function. *Mol Hum Reprod 3*:27–45.

Ingman T, Sorsa T, Suomalainen K, Halinen S, Lindy O, Lauhio A, Saari H, Konttinen YT, Golub LM. 1993. Tetracycline inhibition and the cellular source of collagenase in gingival crevicular fluid in different periodontal diseases. A review article. *J Periodontol 64*:82–88.

Kraulis P. 1991. MOLSCRIPT: A program to produce both detailed and schematic plots of protein structures. *J Appl Crystallogr 24*:946–950.

Li J, Brick P, O'Hare MC, Skarzynski T, Lloyd LF, Curry VA, Clark IM, Bigg HF, Hazleman BL, Cawston TE, Blow DM. 1995. Structure of full-length porcine synovial collagenase reveals a C-terminal domain containing a calcium-linked, four-bladed beta-propeller. *Structure 3*:541–549.

Lovejoy B, Cleasby A, Hassell AM, Longley K, Luther MA, Weigl D, McGeehan G, McElroy AB, Drewry D, Lambert MH, Jordan SR. 1994a. Structure of the catalytic domain of fibroblast collagenase complexed with an inhibitor. *Science 263*:375–377.

Lovejoy B, Hassell AM, Luther MA, Weigl D, Jordan SR. 1994b. Crystal structures of recombinant 19-kDa human fibroblast collagenase complexed to itself. *Biochemistry 33*:8207–8217.

MacDougall JR, Matrisian LM. 1995. Contributions of tumor and stromal matrix metalloproteinases to tumor progression, invasion and metastasis. *Cancer Metastasis Rev 14*:351–362.

Marcy AI, Eiberger LL, Harrison R, Chan HK, Hutchinson NI, Hagmann WK, Cameron PM, Boulton DA, Hermes JD. 1991. Human fibroblast stromelysin catalytic domain: Expression, purification, and characterization of a C-terminally truncated form. *Biochemistry 30*:6476–6483.

Matrisian LM. 1994. Matrix metalloproteinase gene expression. *Ann NY Acad Sci 732*:42–50.

Matthews BW. 1988. Structural basis of action of thermolysin and related zinc peptidases. *Acc Chem Res 21*:333–340.

Merritt EA, Murphy MEP. 1994. RASTER3D Version 2.0, a program for photorealistic molecular graphics. *Acta Crystallogr D 50*:869–873.

Nagase H. 1997. Activation mechanisms of matrix metalloproteinases. *Biol Chem Hoppe Seyler 378*:151–160.

Newby AC, Southgate KM, Davies M. 1994. Extracellular matrix degrading metalloproteinases in the pathogenesis of arteriosclerosis. *Basic Res Cardiol 89* (Suppl 1):59–70.

Ray JM, Stetler-Stevenson WG. 1994. The role of matrix metalloproteases and their inhibitors in tumour invasion, metastasis and angiogenesis. *Eur Respir J 7*:2062–2072.

Saus J, Quinones S, Otani Y, Nagase H, Harris ED Jr, Kurkinen M. 1988. The complete primary structure of human matrix metalloproteinase-3. Identity with stromelysin. *J Biol Chem 263*:6742–6745.

Serni U, Fibbi G, Anichini E, Zamperini A, Pucci M, Mannoni A, Matucci A, Benucci M, Del Rosso A, Del Rosso M. 1995. Plasminogen activator and receptor in osteoarthritis. *J Rheumatol Suppl 43*:120–122.

Snyder RW, Stamer WD, Kramer TR, Seftor RE. 1993. Corticosteroid treatment and trabecular meshwork proteases in cell and organ culture supernatants. *Exp Eye Res 57*:461–468.

Spurlino JC, Smallwood AM, Carlton DD, Banks TM, Vavra KJ, Johnson JS, Cook ER, Falvo J, Wahl RC, Pulvino TA, Wendoloski JJ, Smith DL. 1994. 1.56 A structure of mature truncated human fibroblast collagenase. *Proteins 19*:98–109.

Stams T, Spurlino JC, Smith DL, Wahl RC, Ho TF, Qoronfleh MW, Banks TM, Rubin B. 1994. Structure of human neutrophil collagenase reveals large S1′ specificity pocket. *Nat Struct Biol 1*:119–123.

Stöcker W, Grams F, Baumann U, Reinemer P, Gomis-Ruth FX, McKay DB, Bode W. 1995. The metzincins—Topological and sequential relations between the astacins, adamalysins, serralysins, and matrixins (collagenases) define a superfamily of zinc-peptidases. *Protein Sci 4*:823–840.

Stockman BJ, Walden DJ, Gates JA, Scahill TA, Kloosterman DA, Mizsak SA, Jacobsen EJ, Belonga KL, Mitchell MA, Mao B, Petke JD. 1998. Solution structures of stromelysin complexed to thiadiazole inhibitors. *Protein Sci*. Forthcoming.

Terada T, Kitamura Y, Nakanuma Y. 1997. Normal and abnormal development of the human intrahepatic biliary system: A review. *Tohoku J Exp Med 181*:19–32.

Wetmore DR, Hardman KD. 1996. Roles of the propeptide and metal ions in the folding and stability of the catalytic domain of stromelysin (matrix metalloproteinase 3). *Biochemistry 35*:6549–6558.

Zask A, Levin JI, Killar LM, Skotnicki JS. 1996. Inhibition of matrix metalloproteinases: Structure based design. *Curr Pharmaceut Des 2*:624–661.